Microreactors as a Tool for Acquiring Kinetic Data on Photochemical Reactions

Tristan Aillet, Karine Loubiere, Odile Dechy-Cabaret, Laurent Prat

▶ **To cite this version:**

Tristan Aillet, Karine Loubiere, Odile Dechy-Cabaret, Laurent Prat. Microreactors as a Tool for Acquiring Kinetic Data on Photochemical Reactions. Chemical Engineering and Technology, 2016, 39 (1), pp.115-122. 10.1002/ceat.201500163 . hal-01927694

HAL Id: hal-01927694
https://hal.science/hal-01927694

Submitted on 3 Dec 2021

HAL is a multi-disciplinary open access archive for the deposit and dissemination of scientific research documents, whether they are published or not. The documents may come from teaching and research institutions in France or abroad, or from public or private research centers.

L'archive ouverte pluridisciplinaire **HAL**, est destinée au dépôt et à la diffusion de documents scientifiques de niveau recherche, publiés ou non, émanant des établissements d'enseignement et de recherche français ou étrangers, des laboratoires publics ou privés.

OATAO
Open Archive Toulouse Archive Ouverte

Open Archive TOULOUSE Archive Ouverte (OATAO)
OATAO is an open access repository that collects the work of Toulouse researchers and makes it freely available over the web where possible.

This is an author-deposited version published in : http://oatao.univ-toulouse.fr/
Eprints ID : 15638

To link to this article : DOI:10.1002/ceat.201500163
URL : http://dx.doi.org/10.1002/ceat.201500163

To cite this version :
Aillet, Tristan and Loubiere, Karine and Dechy-Cabaret, Odile and Prat, Laurent E. *Microreactors as a Tool for Acquiring Kinetic Data on Photochemical Reactions.* (2016) Chemical Engineering & Technology, vol. 39 (n° 1). pp. 115-122. ISSN 0930-7516

Any correspondence concerning this service should be sent to the repository administrator: staff-oatao@listes-diff.inp-toulouse.fr

Tristan Aillet[1,2]
Karine Loubière[1,2]
Odile Dechy-Cabaret[1,3]
Laurent Prat[1,2]

[1]Université de Toulouse, INPT, ENSIACET, Toulouse, France.

[2]CNRS, Laboratoire de Génie Chimique, Toulouse, France.

[3]CNRS, Laboratoire de Chimie de Coordination, Toulouse, France.

Microreactors as a Tool for Acquiring Kinetic Data on Photochemical Reactions

For the first time, the application of microreactors as a tool for acquiring kinetic data on a photochemical reaction is demonstrated. For illustration, a T-photochromic system is considered. By using modeling tools and carrying out specific experiments in a spiral-shaped microreactor irradiated by an ultraviolet/light-emitting diode (UV-LED) array, the two kinetic parameters of the reaction, namely, quantum yield and rate of thermal back reaction, are determined. Once these parameters are known, the photochromic reaction is performed in two other microreactors in order to investigate a wider range of operating conditions. It is observed that a critical residence time exists beyond which the conversion into the open form decreases due to a decomposition reaction. The value of the critical residence depends on the microreactor type, which can be predicted by applying the model developed.

Keywords: Kinetic data acquisition, Microreactor, Photochemistry, Photochromic system, Ultraviolet/light-emitting diode

DOI: 10.1002/ceat.201500163

1 Introduction

Organic photochemistry achieves selective transformations with high chemical and quantum yields, and in many cases without chemical activation. The ability to construct strained rings and polycycles literally with a 'flick of a switch' makes photochemistry especially important for the synthesis of complex natural products [1, 2]. Since the photon can be regarded as a "traceless reagent", photochemistry is considered as a green methodology par excellence. Nevertheless, it has not found widespread implementations in the chemical industry [3]. This reluctance is due to currently available technology, which requires outdated batch reactors, often operating in a circulating loop, equipped with energy-demanding mercury lamps. In these photoreactors, process limitations are numerous due to the uncontrolled coupling between hydrodynamics, radiative transfer, mass transfer, and photochemical kinetics. As a result, lower selectivity and yields than on lab-scale are commonly obtained. Furthermore, these systems need large dilutions to overcome unfavorable light absorption, optical filters to cut out undesired wavelengths, and intensive cooling to counter the heat generation by the lamps.

Over the last decades, continuous microstructured technologies have emerged as real alternatives to the batch process, since they enable reaction outcomes to be improved [4]. For photochemistry, they offer additional advantages, such as extensive light penetration even for concentrated chromophore solutions and a control of the irradiation time [5, 6]. Thus, as the increasing number of publications dealing with this field demonstrates, microreactors become a new synthesis tool enabling to easily carry out photochemical reactions under continuous mode and to achieve higher conversion and selectivity than in conventional batch photoreactors while significantly reducing irradiation times [7].

Paradoxically, flow photochemistry studies on industrial scale are still rare. In particular, at present there are few attempts to model the positive effect of the microscale on photochemical reactions from a chemical engineering context. This research gap currently prevents the implementation of photochemical reactions in continuous-flow processes compatible with an industrial production. Motivated by this perspective, our previous works [8–11] have applied different modeling processes, 1D oder 2D, for various photochemical reactions taking into account, if necessary, the polychromatic character of the light source, to predict the conversion at the microreactor's outlet. On this basis, some practical guidelines have been proposed to avoid mass-transfer limitations in microphotoreactors.

In keeping with these works, the present study aims at showing, for the first time, how microreactors can also be used as a tool for acquiring kinetic data on photochemical reactions. For illustration, a T-photochromic system will be considered, involving a reversible reaction between a closed form and an open form. The kinetic parameters of this reaction will be determined using the modeling tools previously developed [8, 9, 11] coupled with specific experiments in a spiral-shaped microreactor irradiated by an ultraviolet/light-emitting diode

Correspondence: Dr. Karine Loubière (karine.loubiere@ensiacet.fr), Université de Toulouse, CNRS, Laboratoire de Génie Chimique (LGC UMR 5503), 4 allée Emile Monso, BP 84234, 31432 Toulouse, France.

(UV-LED) array (Sect. 3). Once these parameters are known, this photochromic reaction will be carried out in two other microreactors in order to investigate a wider range of operating conditions (Sect. 4). The differences obtained between microreactors will be discussed and explained.

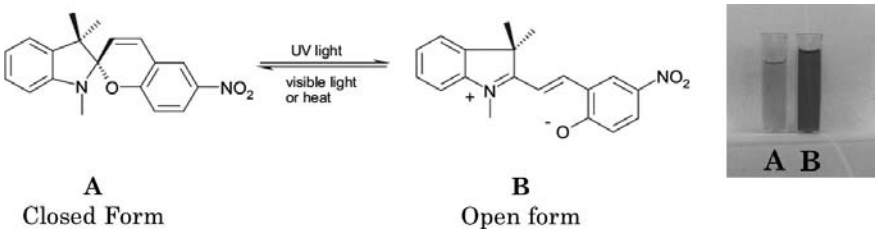

Figure 1. (a) Reversible reaction between the closed and the open forms of TMINBPS; (b) pictures illustrating the difference in color before irradiation (closed form A) and after irradiation (open form B).

2 Experimental

2.1 Photochemical Reaction

The reaction under test is a photochromic system AB ($1k$, 2Φ)[1] involving 1,3,3-trimethylindolino-6'-nitrobenzopyrylospiran, named TMINBPS (#CAS 1498-88-0, 322.36 g mol^{-1}). It involves a reversible bimolecular system where the initial colorless species A, which is the closed form of TMINBPS, is thermally stable and reacts photochemically via a reaction step ($A \xrightarrow{UV} B$) characterized by the quantum yield Φ_{AB}. The species formed B, which is the open form of TMINBPS (pink color), has a short lifetime and transforms into A by two discoloration processes governed by the rate of thermal reaction k_t and the reverse photochemical quantum yield Φ_{BA} (Fig. 1). $\xrightarrow{\Delta}$

The kinetics of the thermal back reaction ($B \xrightarrow{\Delta} A$) mainly depends on the solvent nature and is expressed as a first-order reaction. The open form B is not stabilized in nonpolar solvents, leading to a quick back reaction to the closed form A. On the contrary, using polar solvents enables to increase the lifetime of the open form B to a few minutes. In the present study, ethanol was chosen as solvent for two main reasons: (i) it enables an easy reaction monitoring and data analysis, i.e., sufficiently slow thermal back reaction, and (ii) some data on the rate of the thermal back reaction ($B \xrightarrow{\Delta} A$) in this solvent are available in the literature (see Sect. 3.3).

Hence, the unknown parameters of the photochromic system, defined at a given irradiation wavelength, λ_{irrad}, are: Φ_{AB}, Φ_{BA}, k_t, and and κ_B. The latter parameter is the molar napieran absorption coefficient of the species B; it is considered as unknown because it is impossible to physically isolate the species B due to its transient character (short lifetime).

2.2 Microreactors and Methods

In the present study, two types of microreactors were used. Spiral-shaped microreactors, named SS1 and SS2, consisted of a tube which was inserted inside a channel carved in a flat aluminum plate and wound in a spiral geometry, the inlet of the tube being located at the center of the spiral (Fig. 2 a). They were illuminated by a UV-LED array made by the Led Engineering Development® (Toulouse, France), identical to the one described in [9]. The distance H between the UV-LED array and the fluorinated ethylene propylene (FEP) tube was chosen so as to allow varying the photon flux in a wide range by changing the electrical intensities I_a while ensuring a uniform illumination at the microreactor surface. To verify the latter specification, a light source emission model has been developed. For further information, see [10].

The second type of microreactor was a capillary-tower one, named microreactor CT, identical to the one described by Aillet et al. [8], but with a smaller tube length (Fig. 2 b). It was irradiated by a mercury vapor discharge lamp with a medium-pressure Hg Ba/Sr lamp (125 W, HPK Heraeus®) having the dominant emission line at 365 nm [9].

For both types of microreactors, the tube material was FEP because of its UV-transmission property [12]. Aluminum foil protected the supply syringe and the inlet and outlet sections of the tubing from UV light. The solution to be irradiated was fed into the reactor tubing by a high-pressure syringe pump (neMESYS High-Pressure module, Cetoni®). The flow rates typically varied between 0.05 and 30 mL min^{-1}, leading to Reynolds numbers ranging from 1 to 28 in the microreactor SS1, from 1.3 to 88 in the microreactor SS2, and from 0.5 to 344 in the microreactor CT. Whatever the microreactors and the flow rates, the regime was thus laminar. Tab. 1 summarizes the characteristics of the different microreactors.

Table 1. Characteristics of the microreactors used (SS: spiral-shaped; CT: capillary-tower).

	SS1	SS2	CT
Light source	365-LED	365-LED	MP Hg lamp
H [m]	0.036	0.15	–
d [µm]	508	508	508
L [m]	0.55	8	1
V_r [mL]	0.11	1.62	0.2025

All the experiments were carried out

- in the dark to minimize, if existing, the photochemical back reaction ($B \xrightarrow{vis} A$).
- at room temperature (20 ± 2 °C). For that, in the microreactors SS1 and SS2, the aluminum plate in which the tube was inserted was used as heat sink, and for the microreactor CT, an external cooling unit and a refrigerating water circulator were employed for preventing the heating of the reaction

1) List of symbols at the end of the paper.

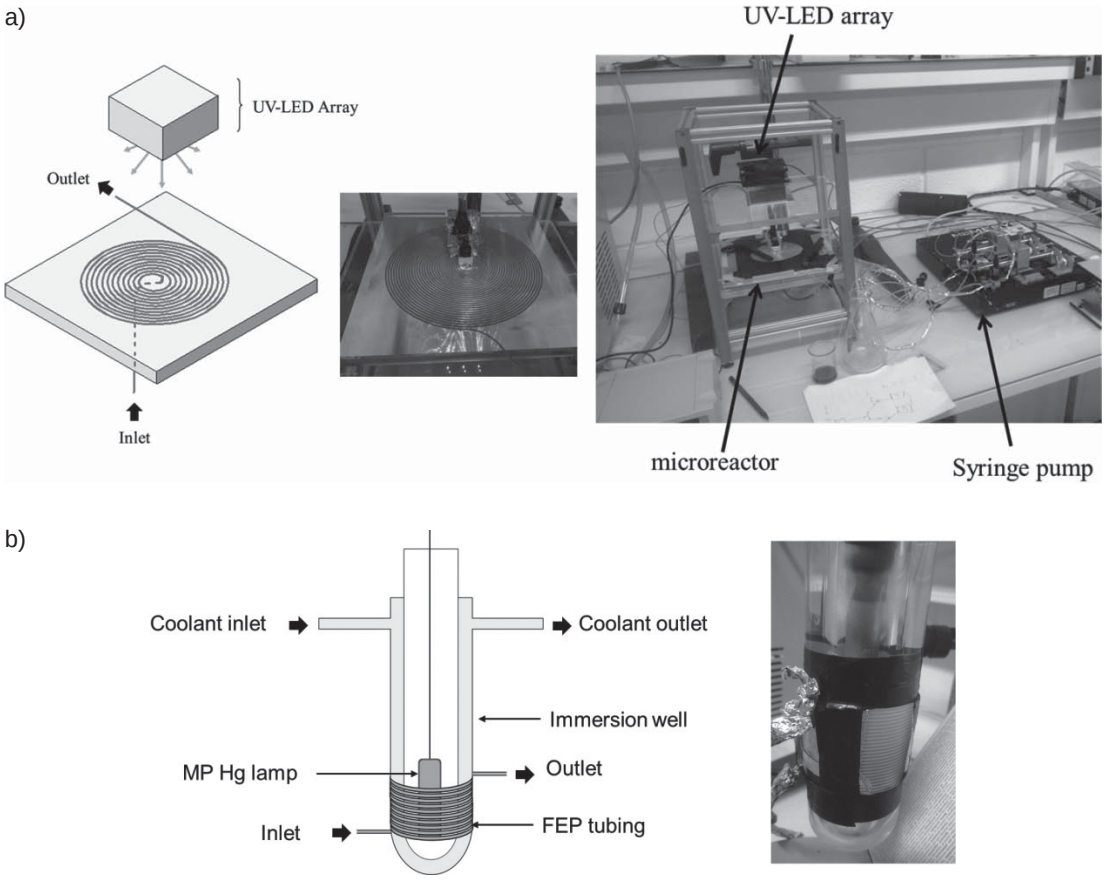

Figure 2. (a) Spiral-shaped microreactor illuminated by the UV-LED array; (b) capillary-tower microreactor illuminated by a medium-pressure mercury lamp.

mixture by the lamp, and thus for keeping it at room temperature.

The methods used for measuring the incident photon flux in microreactors (actinometry) and for the inline reaction monitoring (UV-Vis spectrophotometry) at the outlet of the microreactors are detailed in the Supporting Information (Sect. SI.1).

In Fig. 3, the measured absorption spectrum of the closed form A of TMINBPS is presented. The initial species A strongly absorbs in the UV domain and slightly in the visible domain.

At the irradiated wavelength λ_{irrad} = 365 nm, i.e., the dominant one for the mercury lamp and the single one at which the UV-LED array emits, one finds that

$$\kappa_A^{365} = 1298\ m^2 mol^{-1} \quad (1)$$

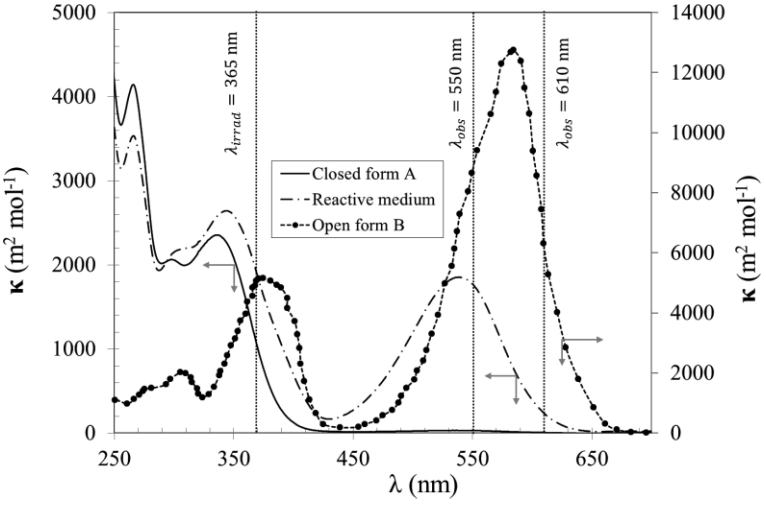

Figure 3. Spectra of molar Napierian absorption coefficients for the closed form A of TMINBPS in ethanol and for the open form B of TMINBPS in ethyl acetate (data reconstructed from [13]).

Fig. 3 also presents the absorption spectrum of the medium when irradiated. As it was not possible to isolate the species B, the absorption coefficients associated with this curve have been calculated with respect to the initial concentration in the closed form of TMINBPS. Thus, these values are not absolute values, as one should rigorously account for the concentrations of the various absorbing species. They are just reported here as a way for illustrating the shape of the absorption spectrum when the medium is irradiated. Firstly, an increase of the absorbance at

365 nm can be observed, thus showing that the species B (open form) also absorbs at the irradiation wavelength. In addition, a peak with a maximum at around 585 nm appears when the medium is irradiated; the evolution of this peak will be used to quantify the formation of the species B. The chosen observation wavelength λ_{obs} will be either 550 nm or 610 nm, depending on the operating conditions (type of microreactor, light source or initial concentration in species A).

3 Identification of Kinetic Parameters

3.1 Literature Background and Modeling Considerations

Many works in the literature, e.g., [13, 14], have suggested that the quantum yield Φ_{BA} of the photochemical back reaction ($B \xrightarrow{vis} A$), if it exists, is low when compared to the one of the forward reaction ($A \xrightarrow{UV} B$). As a consequence, it will be neglected in the present study.

As mentioned in Sect. 2.1, the molar absorption coefficient of the species B (open form), κ_B, is unknown since the species B cannot be isolated. Maafi and Brown [13] have defined an advanced experimental protocol combined with modeling tools for determining, without isolating the species B, κ_B in ethyl acetate as solvent. These values are reported in Fig. 3, leading to

$$\kappa_B{}^{365} = 4550\ m^2 mol^{-1} \quad (2)$$

As the chemical and physical character of ethanol, which is the solvent used in this study, and ethyl acetate is different, some preliminary experiments in ethyl acetate were carried out. They revealed that: (i) neither bathochromic nor hypsochromic shifts on the UV-Vis spectra of the closed form of TMINBPS and of the reactional mixture arose when compared to the ones in ethanol, (ii) the kinetics of the thermal back reaction was very fast within less than 1 min, (iii) the molar absorption coefficient of the species A (closed form) at 365 nm was equal to 1032 $m^2 mol^{-1}$, which is 20 % smaller than in ethanol (Eq. (1)). As the molar absorption coefficient of the species B in ethanol is not reported in the literature, the value of κ_B given in Eq. (2) had to be chosen by default in this study. To take into account the approximation induced by this choice, the influence of this parameter on the determination of kinetic parameters will be studied.

From Eq. (2), the competitive absorbance factor with respect to the species A, β_A, defined by Aillet et al. [11] when the reactant and the product are in competition for absorbing the incident photons, can be calculated at the irradiation wavelength λ_{irrad}, i.e., 365 nm:

$$\beta_A = \frac{\kappa_A}{\kappa_A + \kappa_B} = 0.23 \quad (3)$$

As a consequence, accounting from this literature background, the set of the unknown kinetic parameters can be reduced to Φ_{AB}, the quantum yield of the photochemical forward reaction($A \xrightarrow{UV} B$), and to k_t, the rate of the thermal back reaction ($B \xrightarrow{\Delta} A$). To identify these parameters, some modeling tools have to be developed, coupled with specific experiments in microreactors. These modeling tools are adapted from the model proposed by Aillet et al. [11] in the case of the photochemical reaction $A \xrightarrow{h\nu} B$ where the species A and B are in competition for absorbing the incident photons at a given wavelength. They are detailed in the Sect. SI.2.

3.2 Results

For determining the unknown kinetic parameters (Φ_{AB} and k_t), the spiral-shaped microreactor SS1 irradiated with the 365-nm LED array was used (see Tab. 1). The initial concentration in the closed form A, C_{A0}, was set at 7.76 mol m^{-3}, so as to work in a strong absorbing medium ($A_e{}^0 = 23$).

Fig. 4 a reports the variation of the absorbance at the observation wavelength of 610 nm as a function of the residence time τ_s, for different incident photon fluxes q_p. The absorbance logically becomes higher when τ_s and q_p increase. Fig. 4 b dem-

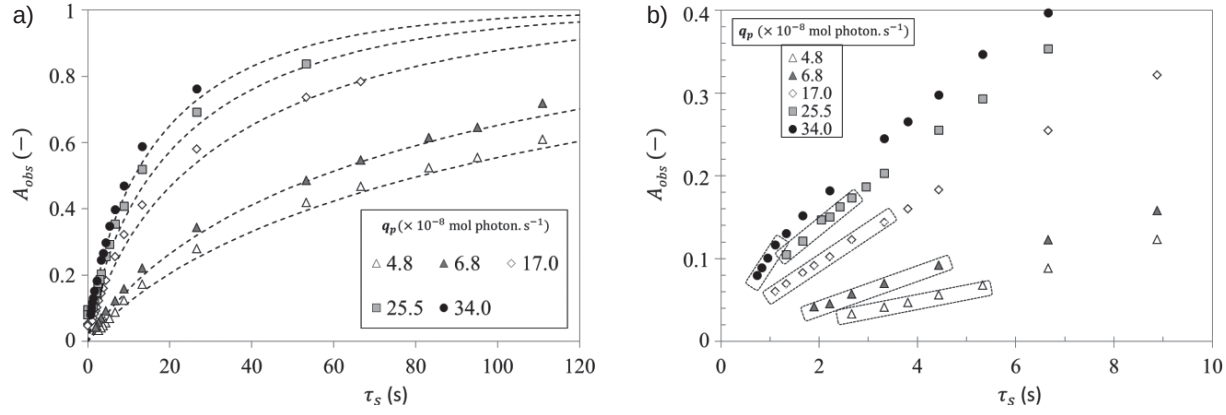

Figure 4. Variation of the absorbance at the observation wavelength of 610 nm with the residence times, τ_s, at different photon fluxes q_p (microreactor SS1): comparison between experimental (symbols) and predicted absorbances (dotted lines). Graphical representation (a) over the whole range of residence times tested, (b) for the smallest residence times; the points surrounded with dotted lines correspond to the ones used to calculate the initial slope of the curve.

onstrates that, for the smallest residence times, A_{obs} varies linearly with τ_s.

By calculating the initial slope of each curve, the parameter $[f_{tube}]q_p$, defined in Eqs. (SI.7–8), can be deduced for each incident photon flux q_p. From this, Fig. 5a can be constructed which shows that the variation of $[f_{tube}]q_p$ with $\frac{q_p}{C_{A0}V_r}$ is linear, thus validating the proposed modeling approach.

According to Eq. (SI.7), the slope of this straight line gives access to $\frac{\Phi_{AB}}{p_{tube}}$:

$$\frac{\Phi_{AB}}{p_{tube}} = 0.267 \quad (4)$$

The rate k_t of the thermal back reaction ($B \xrightarrow{\Delta} A$) is determined by following the decrease of the absorbance at the observation wavelength with time when, after irradiating the reactional medium, the light source and the flow rate in the microreactor are stopped. In Fig. 5 b, the experimental values of $-\ln\frac{A_{obs}}{(A_{obs})_{t=0}}$ are plotted as a function of time. In agreement with Eq. (SI.9), a straight line is obtained, thus confirming that the thermal back reaction ($B \xrightarrow{\Delta} A$) is of first order. From the slope, k_t is calculated:

$$k_t = 3.32\times10^{-4}\ s^{-1} \quad (5)$$

The inverse of this constant corresponds to the characteristic time of the thermal back reaction ($B \xrightarrow{\Delta} A$): one finds 50.2 min.

The order of magnitude of k_t defined in Eq. (5) is in rather good agreement with the one encountered in the literature. Indeed, Roxburgh et al. [15] have experimentally obtained an identical rate of reaction at 21 °C in methanol. Görner [14], Wojtyk et al. [16], and Piard [17] reported the following values in ethanol at 25 °C, respectively: $10^{-3}\ s^{-1}$, $6.9\times10^{-4}\ s^{-1}$, and $6.0\times10^{-4}\ s^{-1}$.

Finally, the parameter p_{tube} (Eq. (SI.5)) is determined by fitting all the experimental absorbances A_{obs}, i.e., for all the photon fluxes q_p and residence times τ_s with the ones predicted by Eq. (SI.4). From this and Eq. (4), the quantum yield is then deduced, leading to the following values:

$$p_{tube} = 0.91$$
$$\Phi_{AB} = 0.24 \quad (6)$$

As illustrated in Fig. 4 a, a good agreement is obtained between experimental and predicted absorbances, whatever the operating conditions. The quantum yield measured by the present method, Φ_{AB} = 0.24 at the irradiation wavelength of 365 nm remains close to the single value found in the literature, namely the one of Görner [14] equal to 0.17 at 354 nm.

As the molar absorption coefficient of the species B was considered by default in ethyl acetate and not in ethanol (see Sect. 3.1), a study has been performed to evaluate the influence of a variation of κ_B on the parameters determined. It was found that when κ_B varies from ± 20 % which corresponds to the order of magnitude of the differences of κ_A in ethyl acetate and in ethanol, it induces the following variations:

- $\beta_A = 0.23 \pm 0.05$
- $p_{tube} = 0.91 \pm 0.11$
- $\Phi_{AB} = 0.24 \pm 0.03$

Thus, even if some approximations are made on κ_B, the consequence on the determined quantum yield remains acceptable with a variation of about 12 %.

4 Implementation of the Photochromic Reaction in other Microreactors

In the previous section, the kinetic parameters characterizing the photochromic system have been determined. From this knowledge, the present section aims at implementing this reaction in other microreactors so as to investigate a wider range of operating conditions.

When the photochromic reaction was carried out in the spiral-shaped microreactor SS1, it has been observed that, whatever the incident photon fluxes, the absorbances at 610 nm increase with the residence times (see Fig. 4 a). Any plateau has been reached, contrary to what one could expect for such a reversible reaction. An in-depth investigation is then required,

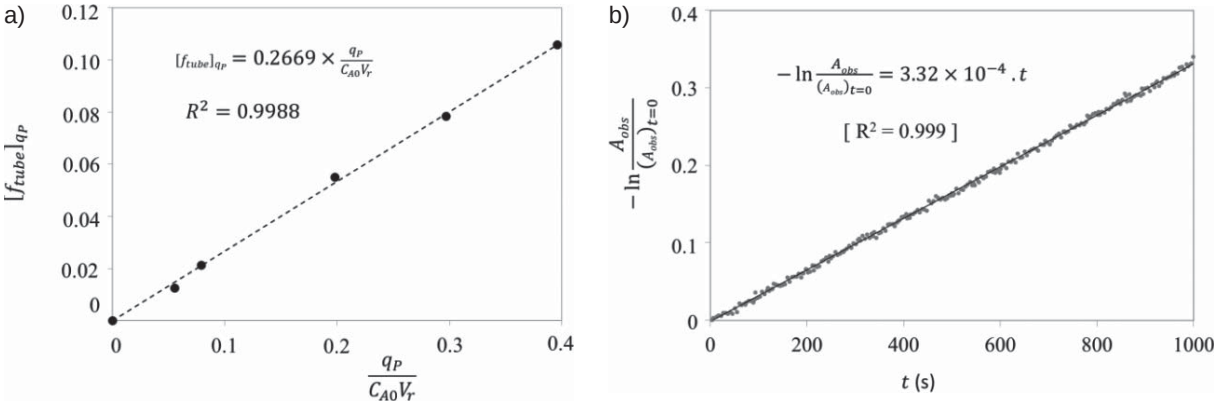

Figure 5. Determination of: (a) the ratio $\frac{\Phi_{AB}}{k_{tube}}$ from the variation of $[f_{tube}]q_p$ with $\left(\frac{q_p}{C_{A0}V_r}\right)$; (b) rate of the thermal back reaction k_t from the variation of $-\ln\frac{A_{obs}}{(A_{obs})_{t=0}}$ with time (microreactor SS1).

in particular for studying the reaction performances for residence times longer than 120 s. For that, a second spiral-shaped microreactor, called SS2, with an identical tube diameter and a greater length (Tab. 1), was used. For ensuring a perfect homogeneity at the microreactor's surface, it was necessary to increase the height H at which the UV-LED array was located (see Tab. 1), leading to a decrease of the incident photon ($q_P = 98.8 \times 10^{-8}$ mol photon s^{-1}; see Supporting Information). The initial concentration in species A, C_{A0}, is kept equal to 7.76 mol m^{-3}.

Fig. 6 presents the variation of the absorbance at the observation wavelength of 610 nm with the residence times. One can observe that a maximal value of the absorbance, A_{obs} = 0.79, is reached for a residence time of almost 389 s. According to Eq. (6) and to Eq. (SI.5), it corresponds to a conversion X of 0.72. For residence times longer than 389 s, the absorbance surprisingly decreases with residence times.

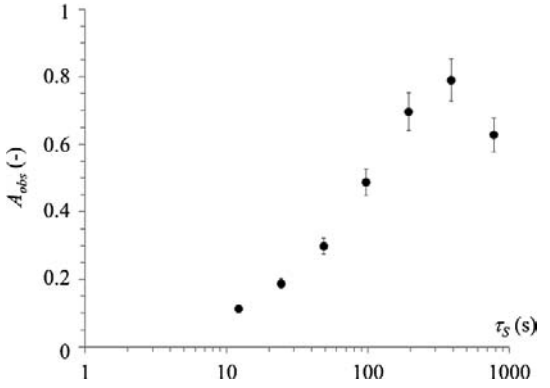

Figure 6. Experiments in the spiral-shaped microreactor SS2 ($q_P = 98.8 \times 10^{-8}$ mol photons s^{-1}): Variation of the absorbance at the observation wavelength (610 nm) with the residence times τ_s (semi-logarithmic scale).

To confirm this phenomenon, the same experiments have been carried out in the capillary-tower microreactor CT irradiated by a polychromatic mercury lamp (see Tab. 1 and Fig. 2 b). The initial concentration in species A is voluntary changed and chosen four times smaller than in the spiral-shaped microreactors: C_{A0} = 1.55 mol m^{-3}. Under such conditions, the observation wavelength has been chosen as 550 nm.

Some typical absorption spectra are presented in Fig. 7 a for different residence times in the microreactor CT. As in the microreactor SS2, a decrease of the peak characteristic of the formation of the species B with the residence times is obtained; in addition, these spectra reveal the apparition of a new peak close to λ = 425 nm, which could be linked to a decomposition of the species B under long irradiation. Fig. 7 b indicates the variation of the absorbance at the observation wavelength (550 nm) with the residence times τ_s. The shape of the curve is identical to the one in the spiral-shaped microreactor SS2. Nevertheless, the critical value of the residence time at which the absorbance is maximal is significantly smaller: it ranges from 1 to 3 s, versus 389 s in the microreactor SS2.

No accurate information has been found in the literature about the decomposition reaction. Possible explanations might be the occurrence of some interactions between the species B and the solvent (ethanol) and/or a photodecomposition of the product. As it was not the main objective of this study, no advanced investigation such as a change of the solvent has been carried out to test these assumptions and/or to attempt the identification of the exact nature, e.g., either photochemical or thermal, of this decomposition reaction. Nevertheless, the kinetics of this decomposition rate seems to be

- significantly slower that the one of the photochemical reaction ($A \xrightarrow{h\nu} B$): the decrease from the maximal absorbance (almost 0.3) to a quasi-null absorbance requires almost 120 s irradiation time whereas an irradiation time of 2 s enables to reach the maximal absorbance (Fig. 7 b);
- faster than the thermal back reaction ($B \xrightarrow{\Delta} A$) whose characteristic time is almost 50 min (Eq. (5)).

To explain the differences in terms of critical residence time, i.e., the one at which the absorbance is maximal, between both microreactors, refer to a previous work [8]. In this work, a methodology has been proposed to compare the performances obtained in two photoreactors 1 and 2, either a batch one or a microreactor, in the case of a photochemical reaction $A \xrightarrow{h\nu} B$. Based on a modeling approach, it has been demonstrated that at a given conversion X the ratio of the residence times, χ_t^X, can be expressed as:

$$\chi_t^X = \frac{\tau_{s,1}}{\tau_{s,2}} = \frac{1}{\chi_\eta^X \times \chi_P} \times \frac{V_{r,1}}{V_{r,2}} \times \frac{C_{A0,1}}{C_{A0,2}} \quad (7)$$

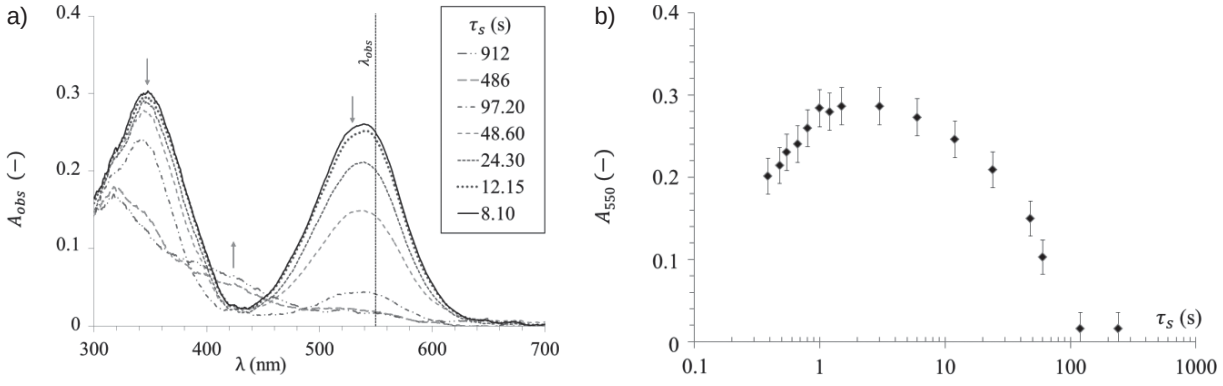

Figure 7. Experiments in the capillary-tower microreactor CT: (a) Absorption spectra of the irradiated medium for different residence times, (b) variation of the absorbance at the observation wavelength (550 nm) with the residence times τ_s (semi-logarithmic scale).

In Eq. (7), ${\chi_\eta}^X$ is the ratio of the photonic efficiencies η^X.

$$ {\chi_\eta}^X = \frac{\eta_1^X}{\eta_2^X} \tag{8} $$

where the photonic efficiency η^X is defined at a given conversion, by:

$$ \eta^X = \frac{X}{X + \frac{1}{A_e^0} \times \ln\left[\frac{1-\exp\left(-A_e^0\right)}{1-\exp\left(-A_e^0(1-X)\right)}\right]} \tag{9} $$

In Eq. (7), χ_P is the ratio of the incident photon flux:

$$ \chi_P = \frac{q_{p,1}}{q_{p,2}} \tag{10} $$

Eq. (7) is applied to the capillary-tower microreactor CT (subscripted with 1) and spiral-shaped microreactor SS2 (subscripted with 2).

The calculation of the average incident photon flux, $\overline{q_{p,1}}$, and of the average absorbance, $\overline{A_{e,1}^0}$, in the capillary-tower microreactor is not direct as the light source is polychromatic. The following values have been obtained: $\overline{q_{p,1}} = 5.99\times10^{-6}$ mol photons s^{-1} and $\overline{A_{e,1}^0} = 45$; see Sect. SI.3 for details. In the microreactor SS2, one obtains $q_{p,2} = 98.8\times10^{-8}$ mol photon s^{-1}, using data reported in Sect. SI.1a, and $A_{e,2}^0 = 23$. This leads to $\chi_P = 6.07$. Considering an arbitrary value of the conversion equal to 0.5, it follows ${\eta_1}^X \approx {\eta_2}^X \approx 1$ (the media are indeed strongly absorbing), thus leading to $\chi_\eta^X = 1$. Using the reactor volumes reported in Tab. 1 and the previously mentioned initial concentration of species 1, it follows:

$$ \begin{cases} \frac{V_{r,1}}{V_{r,2}} = 0.12 \\ \frac{C_{A0,1}}{C_{A0,2}} = 0.2 \end{cases} \tag{11} $$

And finally, with Eq. (7):

$$ \chi_t^X = \frac{\tau_{s,1}}{\tau_{s,2}} = 4.1\times10^{-3} \tag{12} $$

Experimentally, the residences times at which the absorbance is maximal were equal to 2 ± 1 s in the capillary-tower microreactor and 389 ± 2 s in the spiral-shaped microreactor (Figs. 6 and 7); this gives an approximate experimental ratio of 5.1×10^{-3} which is close to the one predicted by Eq. (12). These calculations demonstrate that the increase in the critical residence time observed in the microreactor CT is mainly due to the differences in terms of incident photon flux q_p and of the number of absorbing molecules ($V_r \times C_{A0}$).

5 Conclusions

Promising perspectives are presented for the usage of microreactors as a tool for investigating photochemical reaction kinetics. For illustration, a T-photochromic system was considered. By using modeling tools and carrying out specific experiments in a spiral-shaped microreactor irradiated by a UV-LED array (SS1), the kinetic parameters of the reaction were determined at room temperature. The experiments performed in two other microreactors showed that a critical residence time existed beyond which the conversion into the open form decreased and thus, that a decomposition reaction of the species B occurred. The differences observed in terms of critical residence times between both microreactors were explained due to a modeling approach. In future, some additional investigations will be required to study the influence of the temperature on the kinetic parameters and to understand the exact nature of the decomposition reaction, i.e., the role of the solvent.

The authors have declared no conflict of interest.

Symbols used

${A_e}^0$	[–]	Napierian absorbance; see Eq. (SI.3)
C_{A0}	[mol m^{-3}]	initial concentration in species A
d	[m]	tube diameter
f_{tube}	[–]	parameter defined in Eq. (SI.7)
F_0	[mol photon $m^{-2}s^{-1}$]	photon flux density received at the microreactor wall
k_t	[s^{-1}]	rate of the thermal back reaction ($B \overset{\Delta}{\rightarrow} A$)
H	[m]	height between the UV-LED array and microreactor surface
I_a	[A]	electrical intensities supplying the UV-LED array
L	[m]	length of the reactor
p_{tube}	[–]	parameter defined in Eq. (SI.5)
q_p	[mol photon s^{-1}]	photon flux received in the microreactor
V_r	[m^3]	volume of microreactor
X	[–]	conversion

Greek letters

β	[–]	competitive absorbance factor (see Eq. (3))
κ	[m^2mol^{-1}]	molar Napierian absorption coefficient
λ	[m]	wavelength
η^X	[mol mol photon^{-1}]	photonic efficiency at a given conversion defined
Φ	[mol mol photon^{-1}]	quantum yield
τ_s	[s]	residence time
χ	[–]	ratio of two parameters of same dimension

References

[1] N. Hoffmann, *Chem. Rev.* **2008**, *108 (3)*, 1052–1103.

[2] K. H. Pfoertner, T. Oppenlander, *Ullmann's Encyclopedia of Industrial Chemistry*, Wiley-VCH Verlag, Weinheim **2000**.

[3] A. M. Braun, G. H. Peschl, E. Oliveros, in *CRC Handbook of Organic Photochemistry and Photobiology* (Eds: A. Grisbeck, M. Oelgemöller, F. Ghetti), CRC Press, Boca Raton, FL **2012**, Ch. 1.

[4] K. S. Elvira, X. C. Solvas, R. C. R. Wootton, A. J. de Mello, *Nat. Chem.* **2013**, *5 (11)*, 905–915.

[5] E. E. Coyle, M. Oelgemöller, *Photochem. Photobiol. Sci.* **2008**, *7 (11)*, 1313–1322.

[6] Y. Su, N. J. W. Straathof, V. Hessel, T. Noël, *Chem. Eur. J.* **2014**, *20 (34)*, 10562–10589.

[7] O. Shvydkiv, M. Oelgemoeller, in *CRC Handbook of Organic Photochemistry and Photobiology* (Eds: A. Grisbeck, M. Oelgemöller, F. Ghetti), CRC Press, Boca Raton, FL **2012**, Ch. 3.

[8] T. Aillet, K. Loubière, O. Dechy-Cabaret, L. Prat, *Chem. Eng. Process. Process Intensif.* **2013**, *64*, 38–47.

[9] T. Aillet, K. Loubière, O. Dechy-Cabaret, L. Prat, *Int. J. Chem. React. Eng.* **2014**, *12 (1)*, 1–13.

[10] T. Aillet, *Ph. D. Thesis*, Institut National Polytechnique de Toulouse **2015**.

[11] T. Aillet, K. Loubière, O. Dechy-Cabaret, L. Prat, *AIChE J.* **2015**, *61 (4)*, 1284–1299.

[12] R. H. Feehs, *US Patent 3 554 887*, **1971**.

[13] M. Maafi, R. G. Brown, *Int. J. Chem. Kinet.* **2007**, *39*, 539–545.

[14] H. Görner, *Phys. Chem. Chem. Phys.* **2001**, *3*, 416–423.

[15] C. J. Roxburgh, P. G. Sammes, *Dyes Pigments* **2011**, *90*, 146–162.

[16] J. T. C. Wojtyk, A. Wasey, P. M. Kazmaier, S. Hoz, E. Buncel, *J. Phys. Chem. A* **2000**, *104*, 9046–9055.

[17] J. Piard, *J. Chem. Educ.* **2014**, *91*, 2105–2111.